

# Investigation of Electronic Structure, Mechanical, Magnetic Properties and Thermal Properties of $\text{Co}_2\text{CrSi}_{1-x}\text{Al}_x$ Quaternary Heusler Alloys: An Ab-initio Study

I. Asfour<sup>1,\*</sup>, Soraya Ababou-Girard<sup>2</sup>, Didier Sébilleau<sup>2</sup>

<sup>1</sup>Department of Material Technology, Faculty of Physics, University of Science and Technology Mohamed-Boudiaf, Algeria

<sup>2</sup>Department of Nanosciences Materials, Institute of Physics of Rennes, University of Rennes1, France

Copyright©2019 by authors, all rights reserved. Authors agree that this article remains permanently open access under the terms of the Creative Commons Attribution License 4.0 International License

**Abstract** The structural, electronic and elastic properties of full- Heusler alloys  $\text{Co}_2\text{CrZ}$  ( $Z=\text{Si},\text{Al}$ ) and their quaternary compound  $\text{Co}_2\text{CrSi}_{1-x}\text{Al}_x$ , are determined using the full potential linearized augmented plane waves (FP- LAPW) method based on (GGA) the Generalized Gradient Approximation and density functional theory (DFT) implemented in the WIEN2k package. As results, quaternary compound in  $\text{CuHg}_2\text{Ti}$ -type crystal structure are stable. Density of states (DOS) and bands structure show the existence of energies band gaps in their minority-spin channels with half-metallic behavior. The lattice constant of new quaternary alloys  $\text{Co}_2\text{CrSi}_{1-x}\text{Al}_x$  exhibits a small deviation from Vegard's law and a marginal deviation of the bulk modulus from linear concentration. The three independent elastic constants ( $C_{11}$ ,  $C_{12}$ , and  $C_{44}$ ) are calculated from the direct computation of the stresses generated by small strains. Besides, we report the variation of the elastic constants as a function of pressure as well. From the calculated elastic constants, the mechanical character of  $\text{Co}_2\text{CrSi}_{1-x}\text{Al}_x$  is predicted; elastic constants are calculated to investigate stability criteria and the mechanical nature of the studied materials. The quaternary compound is found to be mechanically anisotropic, ductile and meet the elastic stability criteria. A regular solution model is used to investigate the thermodynamic stability of the alloy which essentially shows a miscibility gap phase by calculating the critical temperatures of the alloys.

**Keywords** FP-LAPW Method, Half-metallic, GGA, DOS, Minority-spin, Spintronic

## 1. Introduction

Fritz Heusler discovered that a type of formula

$\text{Cu}_2\text{MnAl}$  behaves like a ferromagnetic material, although its components are not the magnetic materials in them same .The history of a class of new materials can be traced back to the year 1903[1, 2]. An important classes of materials which are at present under intense study are the so-called half-metals [3]. These materials are hybrids between metals and semiconductors or insulators, presenting metallic behavior for one spin band and semiconducting for the other, and thus overall they are either ferromagnets or ferrimagnets with perfect spin-polarization at the Fermi level [4].

The two compounds  $\text{Co}_2\text{CrSi}$  and  $\text{Co}_2\text{CrAl}$ , these are new innovative materials for many application spintronic. These alloys have a special interest because of their relatively high Curie temperature. The two parents Heusler materials  $\text{Co}_2\text{CrSi}$  and  $\text{Co}_2\text{CrAl}$  proved to be very prospective materials for advanced thermoelectric applications such as in solid-state refrigeration and power generation. Heusler materials are the subject of many studies. This type of material attracts the interest of chemists and physicists of the solid because of their remarkable physical and magnetic properties frequently encountered. Co-based Heusler alloys, which are considered promising candidates for commercial spintronic applications, in particular because of their high Curie temperatures [5].

## 2. Calculation Methodology

The electronic structure calculations based on the generalized-gradient approximation (GGA) are used for the exchange correlation potential [6, 7]. This study is performed using density functional theory DFT [8] calculations within the framework of full-potential linearized augmented plane-wave (FP-LAPW) method as

implemented in WIEN2K package [9, 10]. Such ternary alloys are determined by the generic formulas  $\text{X}_2\text{YZ}$  or  $\text{XYZ}$  [11, 12], is characterized by the formula  $\text{XYZ}$  and called a semi-Heusler alloy. The -Heusler alloys ( $\text{X}_2\text{YZ}$ ) where X and Y are transition metals, and Z is an element of group III, IV or V, in some cases, Y is replaced by either a rare earth element. The  $\text{X}_2\text{YZ}$  Heusler compounds crystallize in the cubic  $\text{L}_{21}$  ( $\text{AlCu}_2\text{Mn}$ -type) structure with the space group  $\text{Fm-}3\text{m}$ . In this structure, X, Y and Z atoms are placed on the Wyckoff positions  $8c$  ( $1/4, 1/4, 1/4$ ),  $4a$  ( $0, 0, 0$ ) and  $4b$  ( $1/2, 1/2, 1/2$ ), respectively. The cubic  $\text{X}_2\text{YZ}$  compounds can also be found in the  $\text{CuHg}_2\text{Ti}$  type structure. This formal  $\text{XYXZ}$ -type structure exhibits  $\text{Td}$  symmetry with the space group  $\text{F-}43\text{m}$ . In that structure, the two X atoms occupy non equivalent positions in contrast to the  $\text{L}_{21}$  structure. This structure is frequently observed when the nuclear charge of the Y element is larger than the one of the X element from the same period, that is  $Z(\text{Y}) > Z(\text{X})$  for two 3d transition metals. In this structure, X atoms occupy the nonequivalent  $4a$  ( $0, 0, 0$ ) and  $4c$  ( $1/4, 1/4, 1/4$ ) positions, while Y and Z atoms are located on  $4b$  ( $1/2, 1/2, 1/2$ ) and  $4d$  ( $3/4, 3/4, 3/4$ ) Wyckoff positions, respectively [13, 21].

The muffin-tin sphere radii  $\text{RMT}$  were chosen as equal to 2.2, 2.4, 1.9 and 1.5 a.u for the Co, Ti, Si and Al atoms, respectively. The plane wave cut-off parameter is taken as  $\text{RMT} \cdot \text{Kmax} = 9$ . The Brillouin zone sampling was performed according to the Monkhorst–Pack scheme and for k-space integration, a  $(14 \times 14 \times 14)$  mesh was used resulting in 104k points of the irreducible part in the Brillouin zone [14]. Study of thermodynamic properties was performed within the quasi-harmonic Debye model implemented in the Gibbs program [15]. The quasi-harmonic Debye model allows us to obtain all thermodynamics quantities from the calculated energy-volume points. Detailed descriptions of this procedure can be found in Refs. [16, 17].

### 3. Results and Discussion

#### 3.1. Structural Properties

In this section, we present the results from the geometrical structure of the quaternary Heusler alloys  $\text{Co}_2\text{CrSi}_{1-x}\text{Al}_x$  as well as the lattice parameter and bulk modulus. To obtain the equilibrium lattice constant and determine the stable structure of these alloys we have performed the structural optimizations for  $\text{Co}_2\text{CrSi}$  and  $\text{Co}_2\text{CrAl}$  alloys for non-magnetic (NM) and ferromagnetic (FM) configurations in their two possible structures  $\text{L}_{21}$  and X-type [5, 22]. From Fig. 1, we can deduce that these

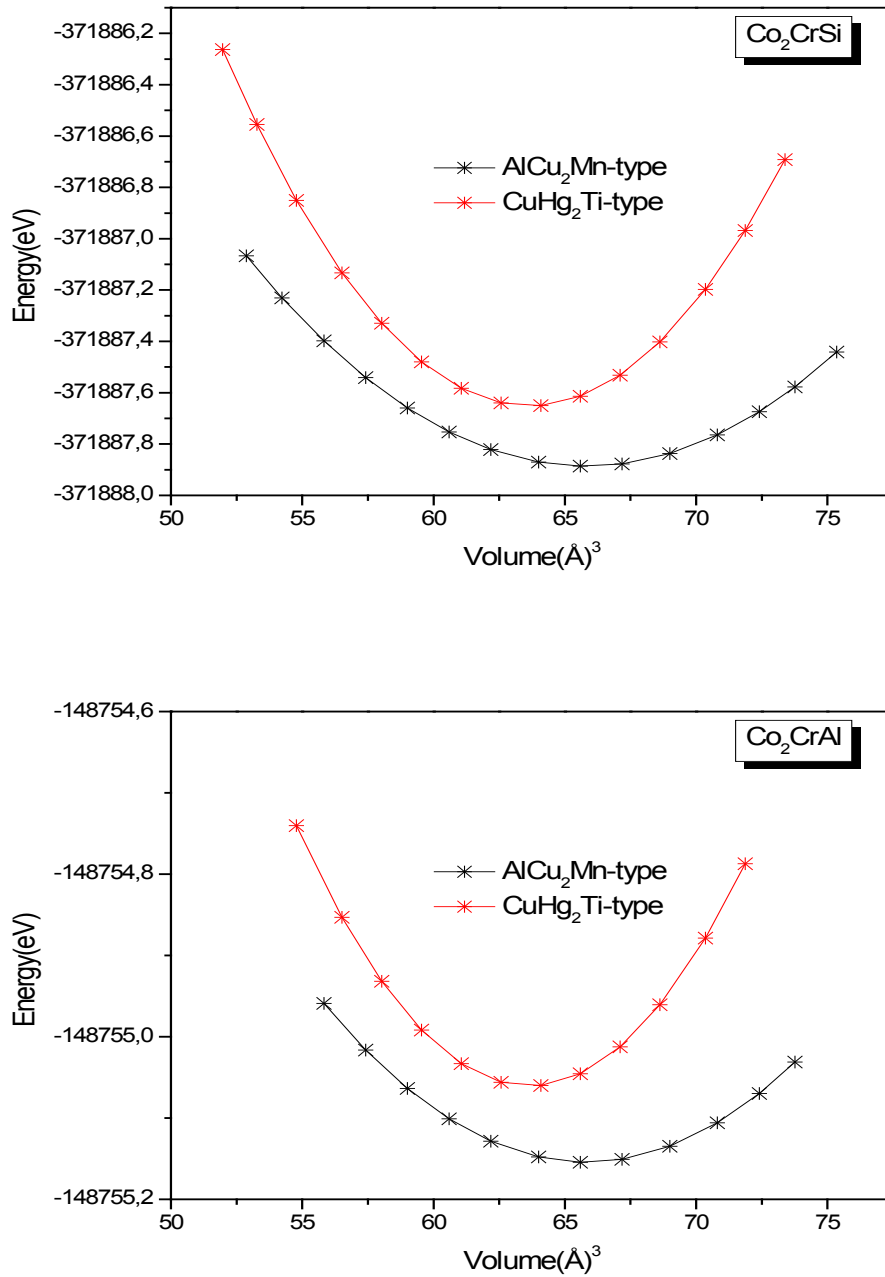
compounds are more stable in the  $\text{L}_{21}$  structure. By means of the empirical Murnaghan equation of state [18], we have fitted the total energy as a function of unit volume to find the corresponding lattice parameters, total energy and bulk modulus. Our results yields a lattice constant of 5.6489 Å and 5.7247 Å for  $\text{Co}_2\text{CrSi}$  and  $\text{Co}_2\text{CrAl}$  compounds, respectively.

To treated the quaternary system for the compositions  $x = 0.25, 0.5$  and  $0.75$ , we have used the supercell model. The Lattice parameters and bulk modulus as a function of composition  $x$  are listed in Table 1. The lattice parameters vary almost linearly following Vegard's law [19, 20] with marginal downward bowing parameters equal to 0.0954 Å. The bulk modulus decreases by going from  $\text{Co}_2\text{CrSi}$  to  $\text{Co}_2\text{CrAl}$  than increases slightly showing a nonlinear behavior. Figs. 2 and 3, show the variation of the calculated lattice parameters and the bulk modulus as a function of the Al concentration for the quaternary alloy. A slight deviation from the Vegard's law is clearly visible for the alloy with bowing upwardly parameter equal to 0.0954 Å, which was obtained by adjusting the calculated values of a polynomial function. On the other hand, the bulk modulus as function of the Al concentration are observed with disorder parameter equal to 5.41 GPa such shows that the incompressibility modulus decreases with increasing the concentration of Al

#### 3.2. Electronic Properties

In the following section, we have analyzed the electronic structure of the  $\text{Co}_2\text{CrSi}_{1-x}\text{Al}_x$  alloys in its stable phase by calculating the total and atomic site-projected l-decomposed densities of states (TDOS and PDOS) for the spins up and down. The calculated TDOS and PDOS for the herein studied alloys are shown in Fig 3. Most transport properties are determined on the basis of knowledge of the density of states. It is clear that the orbital states d of Cr (Co) and the transition metals contribute majorly at the vicinity of the Fermi level. The metallic character is confirmed by the presented majority-spin states. At the minority-spin states, it is seen that there is lack of electronic states at the Fermi level, which reveal the semiconductor character. This finding indicates that our compounds exhibit a half metallic character.

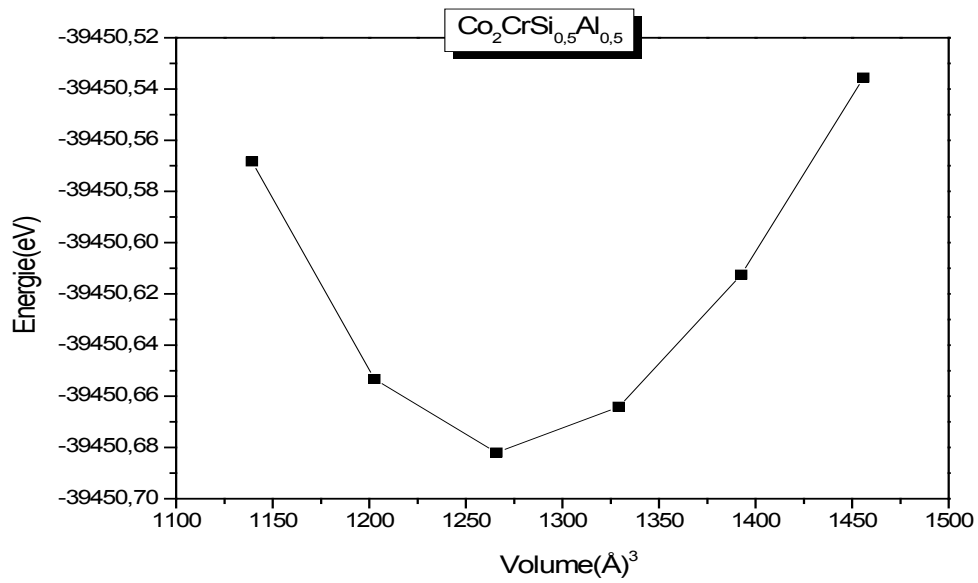
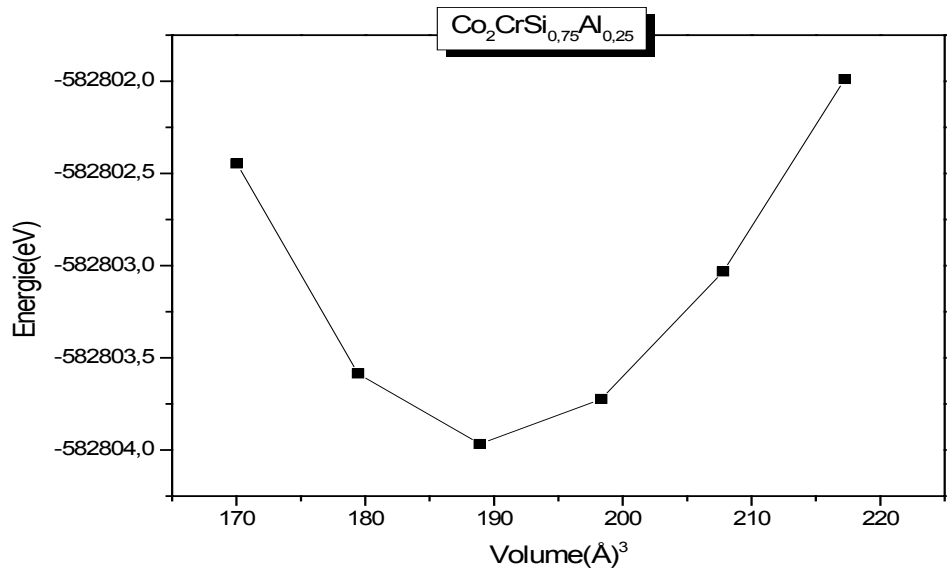
From Fig 3, it is clear that the PDOS present three distinct regions. The first region located between -10 eV and -8 eV below the Fermi level. This region is formed entirely from states 's' of Si and Al, above them, bands are formed with states 'd' of Cr and 'd' of Co localized around -5 eV to -2 eV. The third region 2 eV to 8 eV, the valence bands are dominated by states 'd' of Cr and orbital 'd' of Co.



**Figure 1.** Calculated total energy versus volume curves ferromagnetic (FM) state for AlCu<sub>2</sub>Mn-type and CuHg<sub>2</sub>Ti-type phases of Co<sub>2</sub>CrSi and Co<sub>2</sub>CrAl [5, 22]

**Table 1.** Calculated energy gap Co<sub>2</sub>CrSi<sub>1-x</sub>Al<sub>x</sub> with concentration  $x$  of Al

Compound	$x$	$E_g$ (eV)
Co <sub>2</sub> CrSi <sub>1-x</sub> Al <sub>x</sub>	0.00	0.7228
	0.25	0.7395
	0.50	0.7521
	0.75	0.7602
	1.00	0.7733



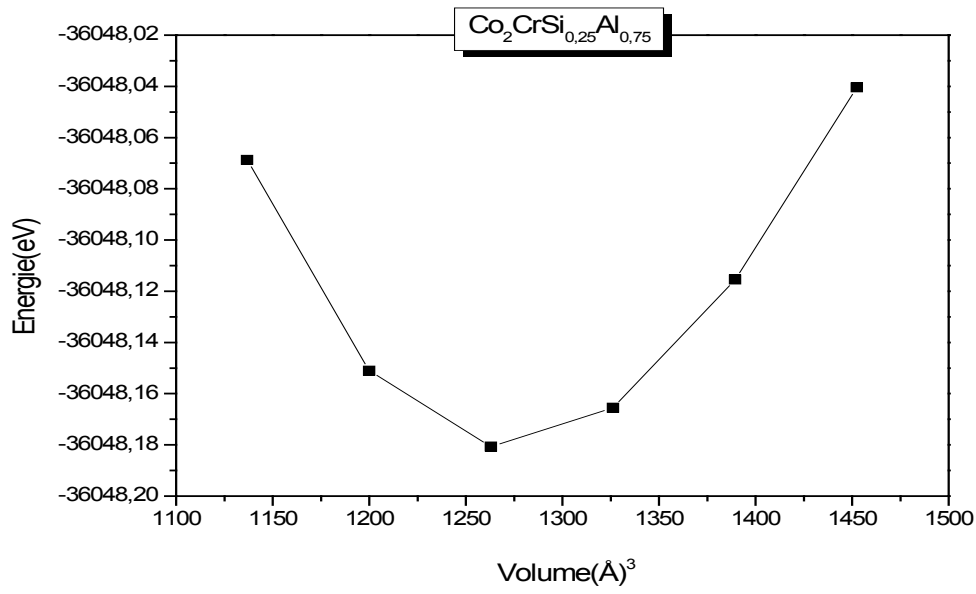
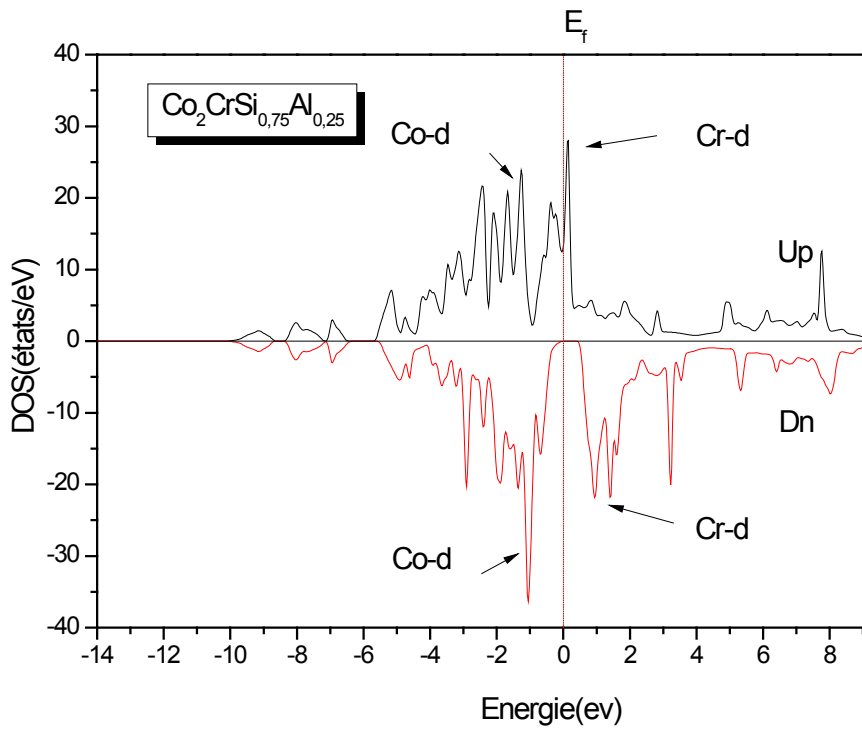
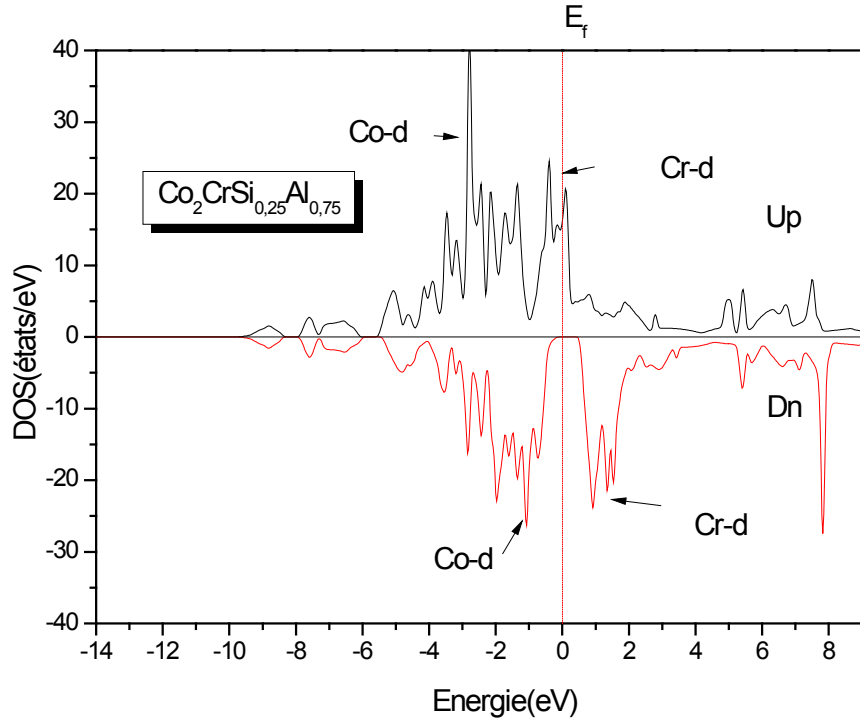
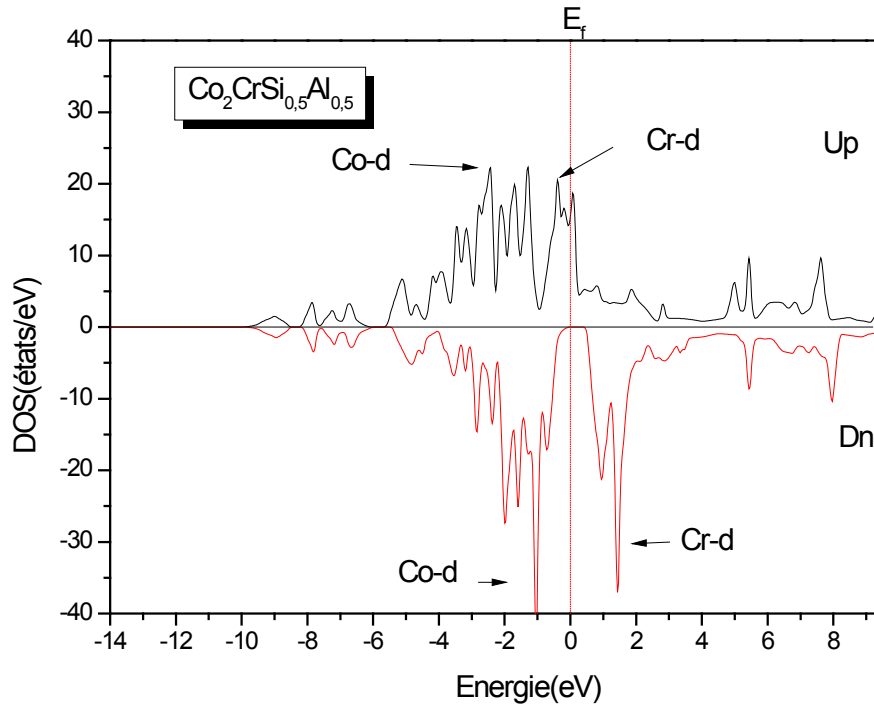


Figure 2. Variation of the total energy as a function of volume for  $\text{Co}_2\text{CrSi}_{1-x}\text{Al}_x$  alloys, a)  $x=0.25$ , b)  $x=0.5$ , c)  $x=0.75$





**Figure 3.** Total and partial density of states of the quaternary Heusler alloys  $\text{Co}_2\text{CrSi}_{1-x}\text{Al}_x$

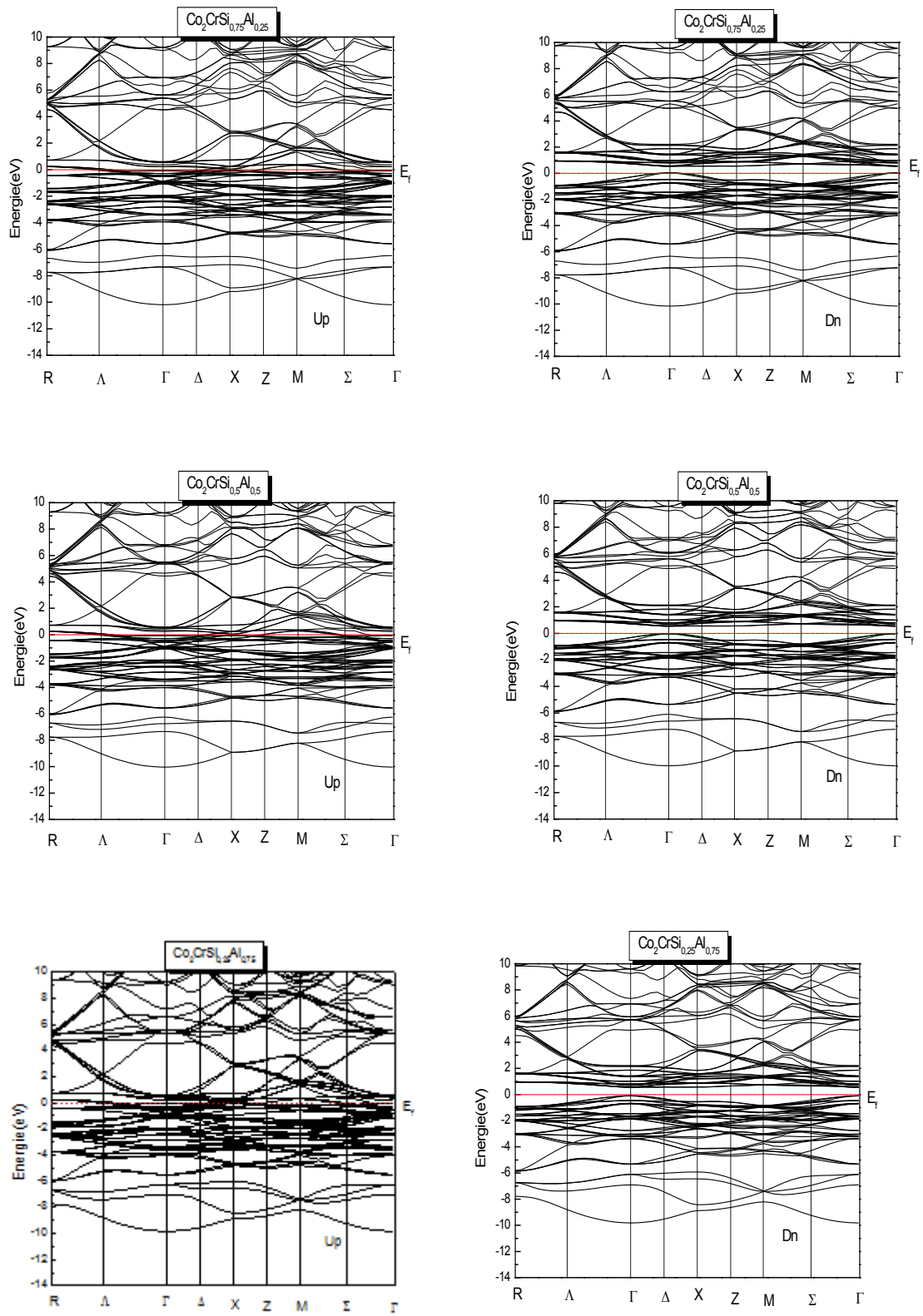


Figure 4. Calculated band structures of the quaternary Heusler alloys  $\text{Co}_2\text{CrSi}_{1-x}\text{Al}_x$

The presence of electronic states is most obvious for the spin up, it is minimal for the spin down and shows the near character semiconductor. In this state, we see a gap between the conduction and the valence band. It can be said that the compounds and their alloys are semiconductors in the state spin-dn. This means that the system has a half-metallic character. We notice a change in indirect gap for quaternary alloy materials studied

The values of the gap energy are summarized in Table 1.

### 3.3. Mechanical Properties

The evaluation of elastic properties is essential to understand the types of atomic bonds and give information on the characteristic between adjacent atomic planes, mechanical stability and anisotropic character of binding. Due to the symmetry of the cubic system of our compounds, the number of elastic constants  $C_{ij}$  is reduced to only three independent constants  $C_{11}$ ,  $C_{12}$  and  $C_{44}$ . More details of the elastic calculation can be found elsewhere. In Table 2, the calculated three independent elastic constants  $C_{11}$ ,  $C_{12}$  and  $C_{44}$ , shear modulus  $G$ , ratio of  $B/G$ , Young's modulus  $E$ , Poisson's ratio ( $\nu$ ), Zener anisotropy factor ( $A$ ), density ( $\rho$ ), longitudinal elastic wave velocities  $V_l$ , transverse elastic wave velocities  $V_t$ , average acoustic velocity  $V_m$ , and Debye temperature ( $\theta_D$ ) of  $\text{Co}_2\text{CrSi}_{1-x}\text{Al}_x$  for various compositions are listed. To our knowledge, we note that there is no result regarding the elastic constants so far available in the literature. Therefore, our results are considered as purely predictive. The traditional mechanical stability conditions in cubic crystals at equilibrium are

expressed in terms of elastic constants as follows:  $C_{11} - C_{12} > 0$ ,  $C_{44} > 0$ ,  $C_{11} + 2C_{12} > 0$  and  $C_{12} < B < C_{11}$  [23]. The computed elastic constants satisfy the above stability criteria, indicating that these compounds are elastically stable. In order to predict the brittle and ductile behavior of materials, Pugh [24] proposed an approximate criterion by the ratio of the critical value that separates brittle and ductile materials is about 1.75. The datas in the Table 2 indicate that the  $B/G$  ratio varies from 3.254 to 3.012, suggesting that of  $\text{Co}_2\text{CrSi}_{1-x}\text{Al}_x$  Heusler alloys are ductile. The Young's modulus  $E$  and Poisson's ratio  $\nu$  are important in technological and engineering application [25]. Young's modulus is defined as the ratio of stress and strain when Hooke's law holds. The Young's modulus of a material is the usual property used to characterize stiffness. The higher the value of  $E$ , the stiffer is the material. From Table 2, the value of the Poisson's ratio is indicative of the degree of directionality of the covalent bonds. Our obtained values for Poisson's ratio vary from 0.3827 to 0.376, which is an indication that the interatomic forces are central forces [26]. From our calculated values of the Zener anisotropy factor  $A$ , which is a measure of the degree of elastic anisotropy of the crystal, we note that our Heusler alloys are elastically isotropic. The Debye temperature is known to be an important fundamental parameter closely related to many physical properties, such as specific heat and melting temperature. At low temperatures, the vibrational excitations arise solely from acoustic vibrations. Hence, at low temperatures, the Debye temperature calculated from elastic constants is the same as that determined from specific heat measurements.

**Table 2.** Calculated lattice constant ( $a$ ), bulk modulus ( $B$ ), pressure derivative of the bulk modulus ( $B'$ ), elastic constants ( $C_{ij}$ ), shear modulus ( $G$ ), ratio of  $B/G$ , Young's modulus ( $E$ ), Poisson's ratio ( $\nu$ ), zener anisotropy factor ( $A$ ), density ( $\rho$ ), longitudinal elastic wave velocities ( $V_l$ ), transverse elastic wave velocities ( $V_t$ ), average acoustic velocity ( $V_m$ ), and Debyetemperature ( $\theta_D$ ) of  $\text{Co}_2\text{CrSi}_{1-x}\text{Al}_x$

	$\text{Co}_2\text{CrSi}_{0.75}\text{Al}_{0.25}$	$\text{Co}_2\text{CrSi}_{0.50}\text{Al}_{0.5}$	$\text{Co}_2\text{CrSi}_{0.25}\text{Al}_{0.75}$
$a(\text{\AA})$	5.6816	5.7097	5.7279
$B(\text{Gpa})$	244.8304	237.6002	225.3246
$B'$	4.1478	4.5647	3.2547
$C_{11}(\text{GPa})$	234.1536	232.2598	268.814
$C_{12}(\text{GPa})$	150.0187	145.8203	177.151
$C_{44}(\text{GPa})$	54.1728	55.2045	55.2045
$G(\text{Gpa})$	54.1827	49.4786	49.4786
$E(\text{GPa})$	138.0081	139.1407	153.782
$\nu$	0.3827	0.3997	0.376
$A$	0.9987	1.0012	1.126
$\rho(\text{g/cm}^3)$	4.2711	4.1163	3.9925
$V_l(\text{m/s})$	14873.543	15456.622	16014.101
$V_t(\text{m/s})$	6213.837	6700.314	7127.841
$V_m(\text{m/s})$	7113.068	7669.945	8159.341
$\theta_D(\text{K})$	776.161	837.522	891.585



**Table 3.** Calculated total and partial magnetic moments (in  $\mu_B$ )  $Co_2CrSi_{1-x}Al_x$

Compounds	Magnetic Moment $\mu_B$					
	Co	Cr	Si	Al	Total	P(%)
$Co_2CrSi$	1.03957 <sup>a</sup>	0.189874 <sup>a</sup>	-0.024-0.02487 <sup>a</sup>	-	4.00003 <sup>a</sup>	100
$Co_2CrSi_{0.75}Al_{0.25}$	1.0166	1.91019	0.01562	-0.00256	3.8011	100
$Co_2CrSi_{0.50}Al_{0.50}$	0.9953	1.9549	0.00630	-0.0031	3.5916	100
$Co_2CrSi_{0.25}Al_{0.75}$	-0.8143	1.3664	0.0460	-0.00307	3.2297	100
$Co_2CrAl$	0.81226 <sup>b</sup>	1.4383 <sup>b</sup>	-	-0.0221 <sup>b</sup>	3.00001 <sup>b</sup>	100

<sup>a</sup>Ref. [22], <sup>b</sup> Ref. [5].

### 3.4. Magnetic Properties

The magnetic moment per formula unit for the alloys of 3d elements can be determined from the number of their valence electrons using Slater–Pauling (SP) rule [27]. According to this rule, magnetic moment for the half metallic moment for the half metallic full-Heusler alloy is given by  $M_f = Z_v - 24$ , where  $M_f$  is the total magnetic moment per unit cell and  $Z_v$  is the total number of valence electrons. The magnetic moment obtained by present calculations is 4.00003  $\mu_B$  and 3.00001  $\mu_B$  for  $Co_2CrSi$  and  $Co_2CrAl$  respectively which agrees well with values from Slater–Pauling rule [27] as well as other calculations [28–30]. The energy band structure of a semi-metallic material has an asymmetry between the spin up states and spins down with a gap or a pseudo energy gap at the Fermi level. This gives rise to the polarizations of the conduction electrons at the Fermi level which may reach 100%.

The calculated total and local magnetic moment for constituent elements are given in Table 3.

It is important to emphasize that, to our knowledge; the scientific community has no experimental or theoretical value of the magnetic moments in these materials.

### 3.6. Thermodynamic Properties

Let us now turn our attention to the phase stability of  $Co_2CrSi_{1-x}Al_x$  quaternary Heusler alloys. For this purpose, we calculate the Gibbs free energy of mixing  $\Delta G_m(x, T)$ , which allows accessing the T–x phase diagram and obtaining the critical temperature  $T_c$ . More details of calculations are given in [31–33] The Gibbs free energy of mixing, for an alloy is expressed as

$$\Delta G_m = \Delta H_m - T \Delta S_m$$

Where

$$\Delta H_m = \Omega x(1-x) \Delta S_m = -R[x \ln x + (1-x) \ln (1-x)]$$

$\Delta H_m$  and  $\Delta S_m$  are the enthalpy and the entropy of mixing,

respectively;  $\Omega$  is the interaction parameter that depends on the material,  $R$  is the ideal gas constant and  $T$  is the absolute temperature. The mixing enthalpy of alloys can be obtained as the difference in energy between the alloy and the weighted sum of the constituents:

$$\Delta H_m = E_{AB_x C_{1-x}} - xE_{AB} - (1-x)E_{AC}$$

Where  $E_{AB_x C_{1-x}}$ ,  $E_{AB}$  and  $E_{AC}$  are the energies of  $AB_x C_{1-x}$ ,  $AB$  and  $AC$  materials, respectively, we calculate  $\Delta H_m$  to obtain the interaction parameter  $\Omega$  as a function of the alloy concentration  $x$ . The variation of  $\Omega$  as a function of the composition  $x$   $Co_2CrSi_{1-x}Al_x$  quaternary, Heusler alloy has been determined Figure. 5. The best fit of our data regarding  $\Omega$  is found to be linear, yielding the following expression:  $\Omega$  (kcal mol<sup>-1</sup>) = 6.127-2.594x.

The average value of the  $x$ -dependent  $\Omega$  in the composition range  $0 \leq x \leq 1$  is estimated to be 6.627 kcal mol<sup>-1</sup>. The larger enthalpy of  $Co_2CrSi_{1-x}Al_x$  alloy suggests a large value of  $\Omega$  and hence a higher critical temperature. Next, in order to determine the stable, metastable and unstable mixing regions of the alloy of interest, we have calculated the temperature–composition phase diagram. Our results are displayed in figure 6. At a temperature lowers than the critical temperature  $T_c$ , the two binodal points are determined as those points at which the common tangent line touches the  $\Delta G_m$  curves. Whereas the two spinodal points are determined as those points at which the second derivative of  $\Delta G_m$  is zero:  $\delta^2(\Delta G_m)/\delta x^2 = 0$ . A critical temperature ( $T_c$ ) value of 1091.0214 K has been evaluated for  $Cr_2NbSi_{1-x}Sn_x$ . The equilibrium solubility limit, i.e. the miscibility gap, is marked by the Spindale curve in the phase diagram. For temperatures and compositions above this curve, a homogeneous alloy is predicted. One can also note the existence of a wide range between spinodal and bimodal curves, thus indicating that  $Co_2CrSi_{1-x}Al_x$  may have a metastable phase. Hence our results indicate that the alloy  $Co_2CrSi_{1-x}Al_x$  is stable at high temperature.

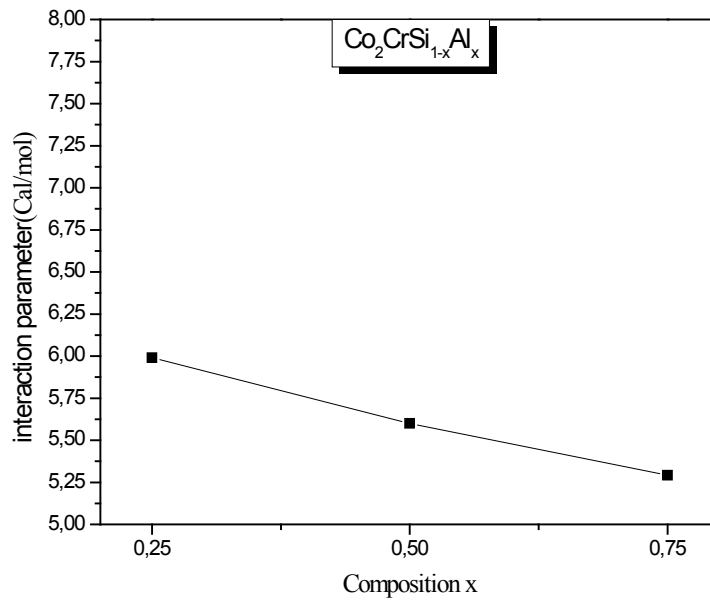


**Figure 5.** Variation of the interaction parameter of  $\text{Co}_2\text{CrSi}_{1-x}\text{Al}_x$  Heusler alloys with Al Concentration

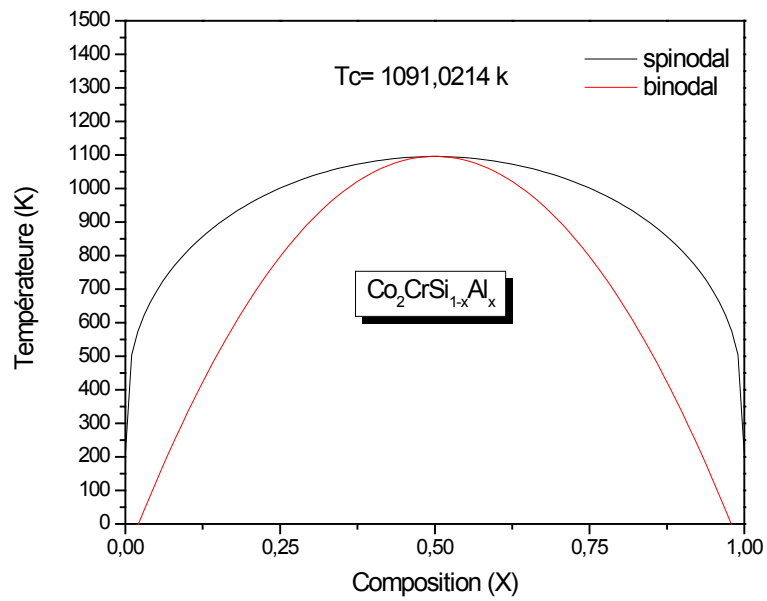


**Figure 6.** T-x phase diagram for  $\text{Co}_2\text{CrSi}_{1-x}\text{Al}_x$  alloys

## 4. Conclusions

The main investigation's goal of this work is to give a report on the structural, elastic and electronic, properties of the quaternary Heusler alloys  $\text{Co}_2\text{CrSi}_{1-x}\text{Al}_x$  at ambient as well as at elevated temperatures. With the linearized augmented plane wave method based on density functional theory and implemented in wien2k code. For exchange correlation potential, we have used the generalized gradient approximation (GGA) of Perdew et al. Our interest in this study was justified by the fact that the properties of these compounds are not available in the literature. The choice of compounds was warranted by the great deal of attention given to these Heusler alloys because of their large field of applications. The electronic band structures show a half-metallic- character our calculated structural parameters are reasonable; also  $C_{11}$ ,  $C_{12}$  and  $C_{44}$  parameters were obtained from calculations. This quaternary Heusler alloy is mechanically stable according to the elastic stability criteria and shows ductile behavior. A linear variation of the lattice constant, elastic constants and Debye temperature with  $x$  has been obtained. The results presented in this paper for the thermodynamic and thermal properties are predictions, and the experiments to prove them are welcomed. Finally, the calculated phase diagram indicated that  $\text{Co}_2\text{CrSi}_{1-x}\text{Al}_x$  is stable at temperature of 1091.0214 K.

## REFERENCES

- [1] F. Heusler, W. Starck, E. Haupt, Verh DPG 5 (1903) 220.
- [2] F. Heusler, Verh DPG 5(1903) 219.
- [3] I.Galanakis, P.H. Dederichs (Eds.), Half-Metallic Alloys: Fundamentals and Applications, in: Lecture Notes in Physics, vol. 676, Springer, Berlin, Heidelberg, 2005.
- [4] I. Galanakis, Ph. Mavropoulos, P.H. Dederichs, J. Phys. D: Appl. Phys. 39(2006) 765.
- [5] I. Asfour, D.Rached, D.Sébilleau, S.Ababou-Girard Universal Journal Physics and Applications. 12(4):59-67, 2018.
- [6] I. Asfour, H. Rached, S. Benalia, D. Rached, J. Alloy. Comp. 676 (2016) 440-451.
- [7] H.C. Kandpal, G.H. Fecher, C. Felser, J. Phys. D: Appl. Phys. 40 (2007) 1507.
- [8] M. Petersen, F. Wagner, L. Hufnagel, M. Scheffler, P. Blaha, K. Schwarz, Computer Physics Communications 126 (2000) 294.
- [9] S.E. Kulkova, S.S. Kulkov, A.V. Subashiev, Computational Materials Science 36 (2006)249
- [10] M.A. Blanco, A. Martín Pendás, E. Francisco, J.M. Recio, R.Franco, J. Mol. Struct. Theochem. 368 (1996) 245.
- [11] E.P. Wohlfarth, K.H.J. Bushow, Ferromagnetic Materials, vol. 4, Elsevier, Amsterdam, 1998.
- [12] H.C. Kandpal, G.H. Fecher, C. Felser, J. Phys. D: Appl. Phys. 40 (2007) 1507.
- [13] F. Heusler, W. Starck, E. Haupt, Verh DPG 5 (1903) 220.
- [14] M.A. Blanco, A. Martín Pendás, E. Francisco, J.M. Recio, R. Franco, J. Mol. Struct.Theochem. 368 (1996) 245.
- [15] E.P. Wohlfarth, K.H.J. Bushow, Ferromagnetic Materials, vol. 4, Elsevier, Amsterdam, 1998.
- [16] M. Flórez, J.M. Recio, E. Francisco, M.A. Blanco, A. Martín Pendás, Phys. Rev. B 66(2002)144112.
- [17] I. Asfour, H. Rached, D. Rached, M. Caid, M. Labair, J. Alloy. Comp. 742 (2018) 736-750
- [18] F.D. Murnaghan, Proc. Natl. Acad. Sci. U.S.A. 30 (1944) 5390.
- [19] L. Vegard, Z. Phys. 5 (1921) 17.
- [20] I. Asfour, H. Rached, S. Benalia, D. Rached, J. Alloy. Comp. 676 (2016) 440-451.
- [21] I. Asfour, H. Rached, D. Rached, M. Caid, M. Labair, J. Alloy. Comp. 742 (2018) 736-750
- [22] I. Asfour, D. Rached, Universal Journal of Mechanical Engineering 6(2) 21-37, 2018.
- [23] F. Chu, Y. He, D.J. Thome, T.E. Mitchell, Scr. Metall. Mater.33 (1995) 1295.
- [24] F.Peng, D.Chen, X.D. Yang, Solid State Commun. 149 (2009) 2135.
- [25] I. Galanakis, P. H. Dederichs, N. Papanikolaou, Phys. Rev. B66 (2002)174429.
- [26] Y. V. Kudryavtsev, N. V. Uvarov, V. N. Iermolenko, J. Dubowik, J. Appl. Phys. 108
- [27] I. Galanakis, P. H. Dederichs, N. Papanikolaou, Phys. Rev. B66 (2002) 174429.
- [28] Y. V. Kudryavtsev, N. V. Uvarov, V. N. Iermolenko, J. Dubowik, J. Appl. Phys.108.
- [29] D. P. Rai, R. K. Thapa, J. Alloys Compd. 542(2012)257.
- [30] S. Ram, M. R. Chauhan, K. Agarwal, V. Kanchana, Philos. Mag. Lett. 91 (2011).
- [31] Swalin R A 1961 Thermodynamics of Solids (New York: Wiley).
- [32] Ferreira L G, Wei S H, Bernard J E and Zunger A 1999 Phys. Rev. B 40 3197.
- [33] Teles L K, Furthmuller J, Scolfaro L M R, Leite J R and Bechstedt F 2000 Phys. Rev. B 62 2475.